International Journal of Pavement Engineering

ISSN: 1029-8436 (Print) 1477-268X (Online) Journal homepage: http://www.tandfonline.com/loi/gpav20

In-situ assessment of the stress-dependent stiffness of unbound aggregate bases: application in inverted base pavements

Efthymios Papadopoulos, Douglas D. Cortes & J. Carlos Santamarina

To cite this article: Efthymios Papadopoulos, Douglas D. Cortes & J. Carlos Santamarina (2016) In-situ assessment of the stress-dependent stiffness of unbound aggregate bases: application in inverted base pavements, International Journal of Pavement Engineering, 17:10, 870-877, DOI: 10.1080/10298436.2015.1022779

To link to this article: http://dx.doi.org/10.1080/10298436.2015.1022779

International Journal of Pavement Engineering, 2016
Vol. 17, No. 10, 870–877, http://dx.doi.org/10.1080/10298436.2015.1022779

Taylor & Francis
Taylor & Francis Group

In-situ assessment of the stress-dependent stiffness of unbound aggregate bases: application in inverted base pavements

Efthymios Papadopoulos[a]*, Douglas D. Cortes[b1] and J. Carlos Santamarina[a2]

[a]*Department of Civil and Environmental Engineering, Georgia Institute of Technology, 790 Atlantic Drive, Atlanta, GA 30332, USA;* [b]*Department of Civil Engineering, New Mexico State University, Room 202, 3035 S. Espina St., Hernandez Hall, Las Cruces, NM 88003, USA*

(*Received 28 October 2014; accepted 21 February 2015*)

Unbound aggregate bases are the primary structural components in many flexible pavements. The response of the unbound aggregate base is critical to the overall performance of the pavement, particularly in inverted base pavements given the proximity of the base to the traffic loads. The behaviour of granular materials such as unbound aggregate bases is inherently nonlinear and anisotropic. An experimental methodology is developed to assess the in-situ stress-dependent small-strain stiffness of unbound aggregate bases under controlled load using wave propagation techniques. CODA wave analysis is used to detect small changes in travel time. The methodology is applied in two distinct case histories of inverted base pavements. Results show that field-compacted granular bases exhibit higher stiffness, lower stress sensitivity and more pronounced anisotropy than laboratory-compacted specimens. The discrepancy in stiffness observed among the two field case histories is primarily attributed to traffic preconditioning sustained by the older pavement. Additional results show that the effect of suction on the stiffness of coarse-grained granular bases is insignificant.

Keywords: unbound aggregate base; inverted base pavement; granular base; pavement; field test; wave propagation; crosshole; uphole; CODA analysis; stiffness

1. Introduction

Stress redistribution within a pavement structure is determined by the relative flexural rigidity between successive pavement layers, i.e. stiffness and thickness (Burmister *et al.* 1943, Burmister 1945, Fox and Fox 1951). Consequently, layer stiffness is an important parameter in the calculation of a pavement's structural capacity (AASHTO 1993, NCHRP 2004).

Unbound aggregate bases support the surface asphalt concrete layers and protect the sub-grade. The stiffness of granular bases is inherently anisotropic and stress-dependent due to their particulate nature (Arthur and Menzies 1972, Roesler 1979, Kopperman *et al.* 1982, Cascante and Santamarina 1996, Santamarina and Cascante 1996, Yimsiri and Soga 2002). There have been only a few attempts to measure the anisotropic stress-dependent stiffness of granular bases in situ (Terrell *et al.* 2003). Yet, the stiffness of granular bases is a critical constitutive parameter for analysis and design, particularly in the case of inverted base pavements due to the proximity of the base to the traffic loads (Cortes and Santamarina 2013, Tutumluer 2013, Papadopoulos and Santamarina 2014).

This study documents an experimental procedure to assess in situ the stress-dependent small-strain anisotropic stiffness of granular bases. Novel field procedures and signal processing techniques are employed. The methodology is applied to two distinct cases of inverted base pavements.

2. Previous studies

The resilient modulus M_r is used to describe the stiffness of pavement layers (Hicks and Monismith 1971). Several laboratory tests have been developed to determine the resilient modulus of granular bases (FHWA 1996, Tutumluer and Seyhan 1999, NCHRP 2002, Puppala 2008). These tests simulate material compaction and loading history relevant to field conditions. However, laboratory compaction does not properly emulate roller compaction, and the stress conditions imposed during resilient modulus tests do not capture the complexity of the stress history and stress field experienced by the granular base under working conditions (Kim and Tutumluer 2005). Furthermore, most tests do not consider the inherent as well as the stress-induced anisotropy of the granular base stiffness which can have a considerable effect on pavement response (Barden 1963, Gazetas 1982, Kim *et al.* 2005, Al-Qadi *et al.* 2010, Wang and Al-Qadi 2013).

Several techniques have been devised for the in-situ measurement of the stiffness of unbound aggregate bases (Fleming *et al.* 2000). Commercially available systems include the falling weight deflectometer (FWD), the light

*Corresponding author. Email: epapadop@gatech.edu

weight deflectometer (LWD) and the seismic pavement analyzer (SPA) (Nazarian *et al.* 1993, Fleming *et al.* 2007, NCHRP 2008). All three methods apply a dynamic load. The first two methods measure surface deflections under an impulse load, while the SPA uses wave propagation and a combination of seismic reflection and SASW measurements. In this case, *P*-wave velocity V_p is related to constrained modulus M_{max} through the bulk density ρ:

$$M_{max} = \rho V_p^2 \quad (1)$$

Similarly, the shear wave velocity is related to shear modulus G_{max}:

$$G_{max} = \rho V_s^2 \quad (2)$$

Recent results confirm the correlation between laboratory and field-measured stiffness values using wave propagation and the resilient modulus of granular bases in the field (Williams and Nazarian 2007, Schuettpelz *et al.* 2010).

However, there are several limitations with conventional in-situ testing techniques. First, the state of stress in the pavement is unknown. Second, most conventional methods do not consider the anisotropic stiffness properties of the unbound aggregate base. Third, the interpretation of boundary measurements conducted at the pavement surface requires inverse problem solving to estimate the stiffness of the pavement layers. Fourth, inversion propagates measurement errors and increases the uncertainty of the inferred values (Santamarina and Fratta 2005).

On the other hand, the small-strain stiffness of the material can be directly measured in situ using seismic methods under controlled loading conditions. For example, Terrell *et al.* (2003) embedded several three-dimensional accelerometers within the unbound aggregate base during pavement construction, and later conducted seismic tests to measure the horizontal and vertical shear wave velocity under different surface loads. The present study is based on *P*-wave propagation in cross-hole and up-hole configurations conducted under controlled surface load to measure the anisotropic stress-dependent stiffness of the unbound aggregate base.

3. Experimental configuration

Two test configurations are implemented to properly characterise the anisotropic stress-dependent stiffness in granular bases. The up-hole and cross-hole techniques, shown in Figure 1, are both based on *P*-wave propagation and require the installation of sensors in the unbound aggregate base.

3.1. *Perforation*

Small-diameter boreholes were drilled in the pavements using several drilling techniques and borehole diameters. Results showed that a 16 mm (5/8″) diamond core drill bit is able to effectively advance the hole with causing minimal material disturbance and without triggering borehole instability.

3.2. *Cross-hole*

The cross-hole configuration is selected to measure the horizontal stiffness (Figure 1a). A piezocrystal is placed in each borehole to form a source–receiver pair. The perforation is filled with high viscosity oil (cP = 320 -

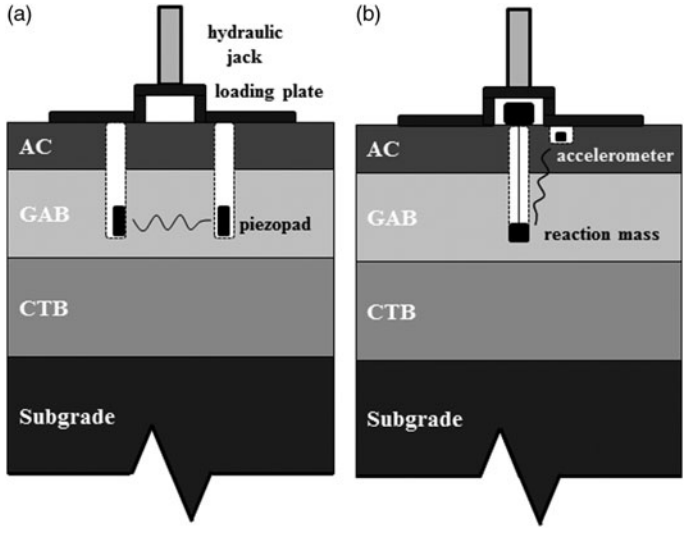

Figure 1. Schematic representation (not to scale) of (a) the cross-hole and (b) the up-hole tests designed to measure the directional stiffness of the granular base. The contact stress is applied using a hydraulic jack acting on a circular plate.

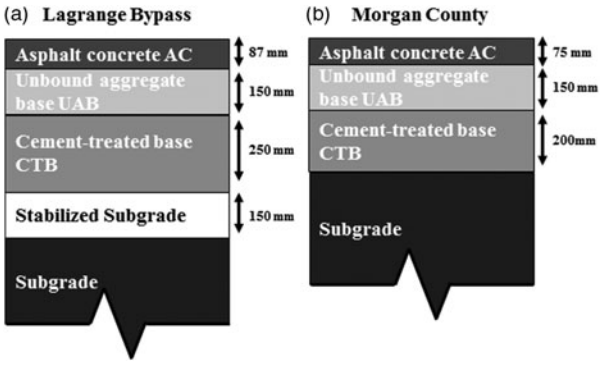

Figure 2. Inverted base pavement structures tested in this study: (a) Lagrange, GA and (b) Morgan County haul road in Buckhead, GA.

mPa s) to stabilise the walls and to couple the piezocrystals with the unbound aggregate base material. The high viscosity of the oil combined with the low permeability of the unbound aggregate base prevents leakage during the course of the test. The source crystal is connected to a signal generator, while the receiver is connected to a preamplifier and a digital storage oscilloscope.

3.3. *Up-hole*

The up-hole configuration is used to determine the vertical stiffness of the base. The piezoelectric actuator is coupled through an aluminium rod with a reaction mass that transmits the vibration to the bottom of the hole (Figure 1b). The rod is acoustically isolated from the perforation walls to prevent spurious signals. A piezoelectric accelerometer embedded and coupled with the asphalt concrete acts as the receiver. The actuator is connected to a signal generator and power amplifier, while the accelerometer is connected to a signal conditioner and finally to a digital storage oscilloscope.

3.4. *Loading configuration*

A 300 mm diameter steel circular loading plate is placed on the pavement surface in order to serve as the loading platform. The vertical force on the plate is applied through a hydraulic actuator that reacts against the frame of a loaded dump truck. The loading is imposed in stages and wave propagation data are recorded at each loading and unloading stage.

4. Case studies: Lagrange and Morgan County

The methodology described above was used to characterise the unbound aggregate base layer at the two inverted base pavements in Georgia (Figure 2). The one in Lagrange (tested on 28 August 2013) involves an 87 mm asphalt concrete layer, a 150 mm unbound aggregate base and a 250 mm cement-treated base. Construction and material properties are documented in Cortes and Santamarina (2013). The second case is the haul road for the Morgan County quarry operated by Martin Marietta Aggregates (tested on 27 September 2013). It consists of a 75 mm asphalt concrete layer, a 150 mm unbound aggregate base and a 200 mm cement-treated base. This pavement was previously tested by Terrell *et al.* (2003). The properties of the unbound aggregate bases tested are summarised in Table 1. Results from the two tests are summarised next.

4.1. *Wave signatures*

Figures 3 and 4 show a typical signal cascades obtained during cross hole test and up hole tests. Travel time decreases and stiffness increases with increasing contact stress. Changes in travel time between consecutive signals are very small and hinder the accurate determination of wave velocity base on first arrival. The innovative signal-processing method used in this study to infer wave velocities is presented next.

Table 1. Index, mechanical and construction properties for the unbound aggregate bases tested during this study.

Morgan County		Lagrange	
Maximum dry density $\rho_{d,max}$ (kg/m^3)	2193	Maximum dry density $\rho_{d,max}$ (kg/m^3)	2190
Optimum water content w_{opt}	6.7%	Optimum water content w_{opt}	7.1%
Mean grain size D_{50} (mm)	6.5	Mean grain size pre-compaction $D_{50,\ pre}$ (mm)	4.5–6.0
D_{10} (mm)	0.1	D_{10} (mm)	0.1
Uniformity coefficient C_u	100	Uniformity coefficient C_u	85
Liquid limit	Non-plastic	LA abrasion loss	49%
Fines content	7%	Fines content	8.5%
Plastic limit	Non-plastic	Median particle principal axis inclination after compaction (°)	20
USCS class	GP–GW	Shear wave velocity V_s (m/s)	200–400

Notes: Data is from Terrell (2002), Cortes and Santamarina (2013) and Papadopoulos (2014). V_s calculated from surface waves measurement at zero overburden stress.

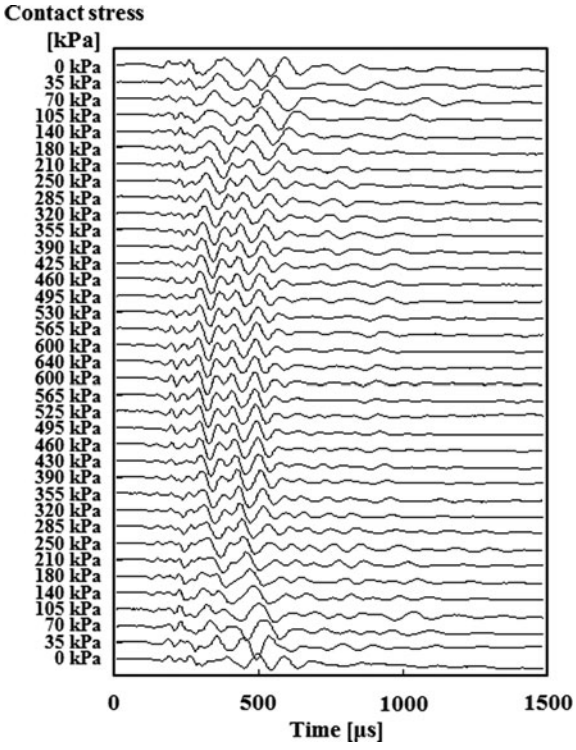

Figure 3. Typical signal cascades for the cross-hole test (Morgan County test). The applied contact stress is noted on the left.

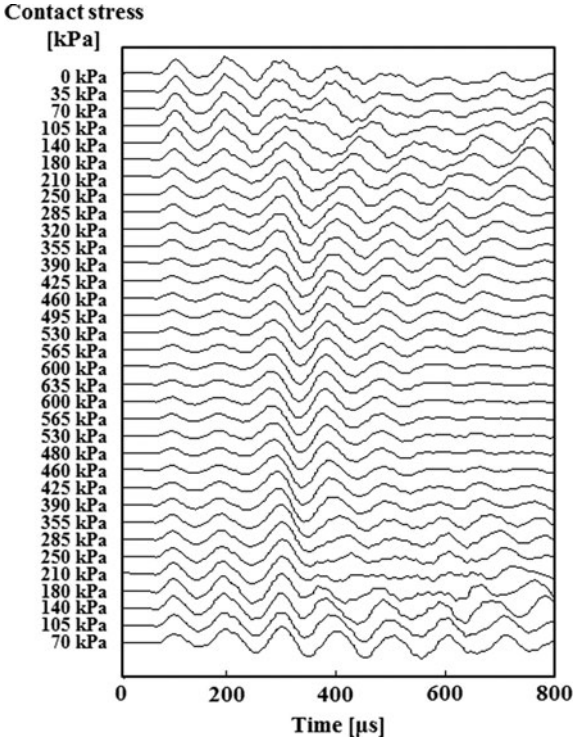

Figure 4. Typical signal cascades for the up-hole test (Morgan County Test). The applied contact stress is noted on the left.

4.2. *CODA wave analysis*

CODA wave interferometry can detect minute changes in signals gathered during process monitoring (Snieder *et al.* 2002, Snieder 2006). CODA analysis assumes that the signal tails correspond to indirect travel paths. The distance travelled along these paths is longer than the direct path responsible for the first arrival; therefore, the effect of any changes in the medium stiffness is magnified. Figure 5a shows the superposition of two waveforms recorded at different stress levels during the Morgan County test. While the change in the first arrival between the 'slow' and the 'fast' signals is almost impossible to discern, the increasing 'offset' between the two signals with time can be used to infer the change in travel time.

CODA analysis can be implemented using time or frequency domain operations (Dai *et al.* 2011). The time-stretched cross-correlation method is employed in this study. First, the time values of the 'slow' signal are multiplied by a constant λ. Second, the cross-correlation between the 'stretched slow' signal and the 'fast' signal is computed. Third, the previous two steps are repeated for different values of λ to identify the λ-value that produces the highest cross correlation (Figure 5b). The optimal λ represents the ratio of travel times between the two original signals. The process is repeated for all signals to determine successive time ratios λ. Last, the signal with

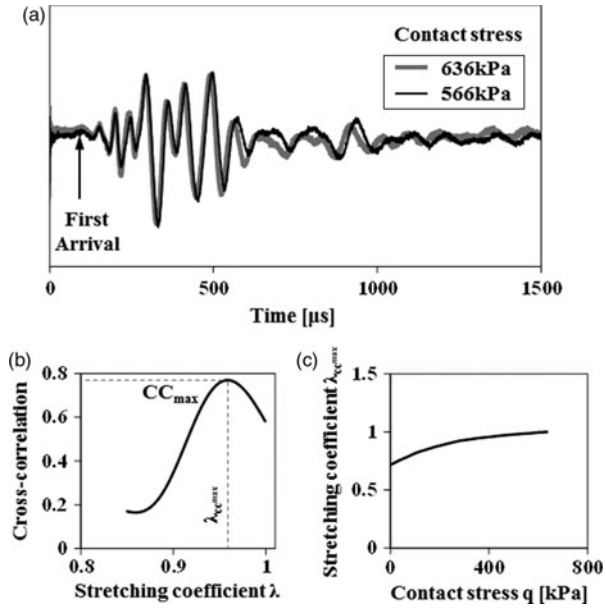

Figure 5. CODA wave analysis: (a) comparison between two consecutive signals (from the cross-hole test at the Morgan County site); (b) cross-correlation versus the stretching coefficient λ for the two signals shown in frame a; (c) stretching coefficient corresponding to maximum cross-correlation values versus all measured signals applied contact stress q.

the clearest first arrival is selected to determine the base travel time t_{base}, while other travel times are inferred from the λ-values as $t_i = \lambda_i \cdot t_{base}$. Figure 5c shows the evolution in the stretching coefficient λ with applied contact stress q for the cross-hole test conducted in Morgan County.

4.3. *Wave velocity*

Horizontal and vertical wave velocities are computed using travel times determined through CODA analysis. For the up-hole test, the *P*-wave velocity in the unbound aggregate base is calculated by subtracting the travel time in the asphalt concrete H^{AC}/V^{AC}:

$$V_p^{GAB} = \frac{H^{GAB}}{\Delta t - H^{AC}/V^{AC}} \quad (3)$$

Equation (3) presumes that the *P*-wave velocity of the asphalt concrete remains constant during the test.

Computed velocities are plotted versus the contact stress q during loading and unloading in Figure 6. *P*-wave velocity increases with increasing contact stress in both cases. The maximum contact stress at the Lagrange site was limited by the truck weight. Both pavements show no hysteresis in stiffness between loading and unloading, which suggests that both granular bases behave elastically, albeit with a nonlinear stress-dependent stiffness.

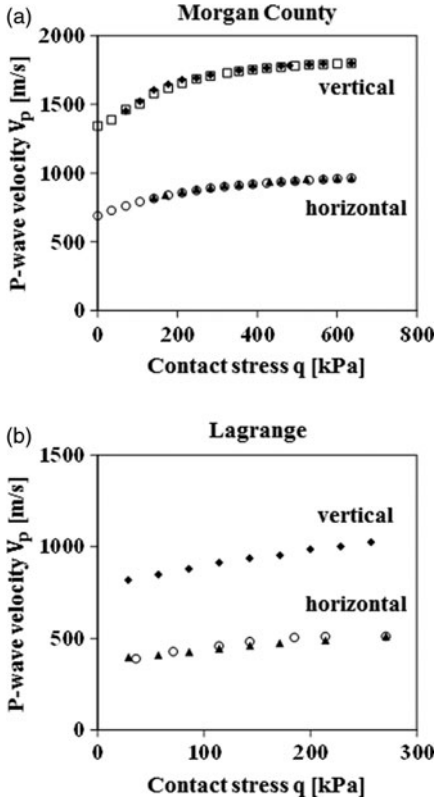

Figure 6. Vertical and horizontal *P*-wave velocity versus contact stress q at the two sites (a) Morgan County and (b) Lagrange. Filled and empty symbols correspond to loading and unloading, respectively.

Velocity values are considerably larger for the Morgan County pavement than the Lagrange pavement. Conditioning of the base due to repetitive loading can explain the discrepancies: the Lagrange section was constructed in 2009 and has been opened to traffic for only the past 2 years (Lewis *et al.* 2012). On the other hand, the Morgan County pavement has been in service for over 12 years and has experienced more than 10^6 ESALs (Lewis *et al.* 2012). Furthermore, similar discrepancy is observed between wave velocities obtained for the Morgan County section during the current study in 2013 and in the previous test conducted in 2002: in the 2002 test, measured velocities were 30–50% lower compared to values measured in this study.

5. Analyses

5.1. *Determination of the state of stress*

The determination of the stress-dependent stiffness requires knowledge of the state of stress within the layer; at the same time, the determination of the state of stress requires knowledge of material stiffness. Due to the interdependency between stress and stiffness, the determination of the stress-dependent stiffness is achieved through successive forward simulations using a numerical model built on the finite element code Abaqus. The constitutive model used and the associated model parameters are reviewed in Papadopoulos and Santamarina (2015). Simulations are iterated until the calculated wave velocity matches the measured values for the given external contact stress. The measured *P*-wave velocity V_p is then plotted versus the respective numerically inferred stress at the centre of the propagation path for both horizontally and vertically propagating waves (Figure 7).

At the same stress, differences between vertical and horizontal stiffness reflect the inherent fabric anisotropy. The ratio of vertical to horizontal stiffness varies between 2 and 4.This ratio is considerably larger than the results of laboratory tests from the same material (Papadopoulos 2014) and highlights the differences between field and laboratory compaction conditions. Furthermore, the slope of the velocity–stress line is different for horizontal and vertical propagation, which indicates differences in stress sensitivity between the vertical and horizontal stiffness (Figure 7). The high fabric anisotropy encountered in field-compacted granular bases has been related to particle share (Kim *et al.* 2005), as well as the in-situ compaction process, which preferentially aligns particles and affects the distribution of contacts (Cortes and Santamarina 2013).

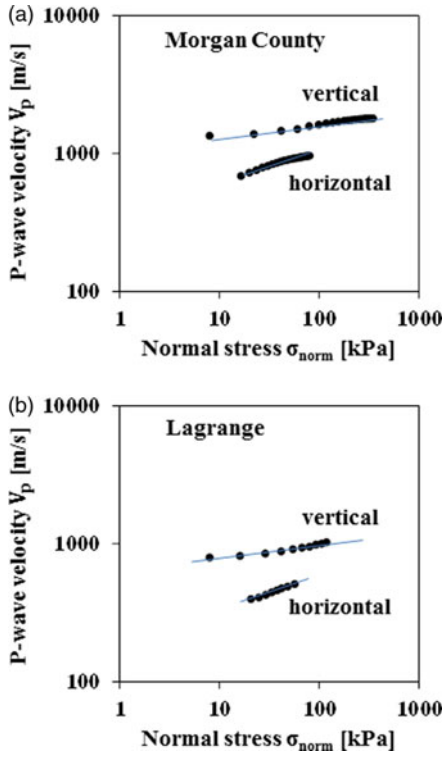

Figure 7. Variation in vertical and horizontal *P*-wave velocity versus the calculated normal stress in the propagation direction σ_{norm} for the two test sites: (a) Morgan County and (b) Lagrange.

5.2. *Laboratory vs. field measurements – discrepancies*

The *P*-wave velocity is sensitive to the normal stress in the direction of wave propagation σ_{norm} and follows a power law (Kopperman *et al.* 1982, Santamarina and Cascante 1996, Santamarina *et al.* 2001):

$$V_p = \alpha\left(\frac{\sigma_{norm}}{kPa}\right)^{\beta} \quad (4)$$

where σ_{norm} is the normal stress at the propagation direction, the α-factor is the value of V_p at 1 kPa and the β-exponent captures the sensitivity of V_p to stress. Computed α and β parameters are plotted together with an extensive data-set of values obtained for a wide range of soils and jointed rocks (Figure 8). Field-compacted unbound aggregate base α and β parameters are similar to values for jointed rocks and higher than α and β values for soils. Thus, at the same stress, field-compacted granular bases exhibit higher stiffness than soils.

Furthermore, field-compacted specimens have higher α and lower stress sensitivity β than laboratory-compacted specimens of unbound aggregate bases. Granular bases in the field have been subjected to high compaction loads as well as heavy traffic during their service life. The heavy loads have resulted in asymptotically stabilising contact crushing and particle rearrangement (McDowell *et al.* 1996, Einav 2007, Hossain *et al.* 2007); these contact-level processes lead to high α-factors and low β-exponents.

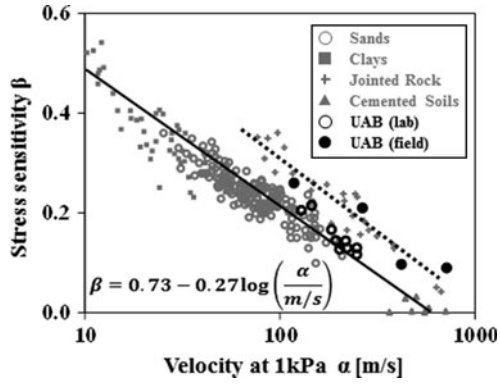

Figure 8. Velocity–stress parameters α and β. Black hollow circles correspond to values obtained from laboratory-compacted specimens, while filled black circles show results for field-compacted unbound aggregate bases. Grey points are data for a wide range of soils collected from the literature (re-plotted from Cha *et al.* 2014).

6. Suction effects

The stiffness of unsaturated granular layers is sensitive to changes in moisture content due to the development of matric suction (Cho and Santamarina 2001, Yuan and Nazarian 2003, Siripun *et al.* 2011). In the absence of fines, the air entry value is a good indicator of the potential effect of suction on the 'equivalent effective stress' which affects stiffness (Alonso 2003, Lu and Likos 2004, Alonso *et al.* 2012). The air entry value reported for the unbound aggregate base in Morgan County is less than 5 kPa (Terrell 2002). At the same time, the calculated values of matric suction range between 11 kPa and 20 kPa, for water contents between 4.8% and 5.7% (Terrell 2002). Therefore, moisture has a minimal effect and the applied load and inherent fabric control the stiffness of unbound aggregate bases with no fines.

7. Conclusions

Two field configurations were developed to determine the stress-dependent stiffness and anisotropy of as-built unbound aggregate bases in pavements. The testing methodology was applied to the two inverted base pavements built in Georgia. Salient observations follow:

- The stiffness of field-compacted granular bases is anisotropic and elastic, but nonlinear and stress-dependent. Both granular bases tested were in the resilient regime.
- The stress-dependent stiffness of granular bases renders the simultaneous determination of the state of stress and stiffness within the pavement an

iterative process in order to extract the constitutive relationship that links the two.

- CODA wave analysis is a robust signal-processing technique for the accurate determination of the stiffness–stress response of granular bases in situ.
- Field-measured stiffness values are considerably higher than values measured on laboratory-compacted specimens. In particular, field-compacted unbound aggregate bases have higher initial stiffness (α-factor) and lower stress sensitivity (β-exponent) than laboratory-compacted specimens. The differences are attributed to the placement and compaction processes, as well as the extensive preconditioning sustained by the field material through traffic and weather cycles. The α and β parameters of field-compacted unbound aggregate bases are close to those of jointed rocks, indicating a very stiff material.
- Suction has a minor effect on the stiffness of granular base, when the aggregate is crushed rock with limited fines content.

Acknowledgements

This work was supported by the Georgia Department of Transportation and the Georgia Construction Aggregate Association under its Executive Director John Cardosa. Additional support was provided by the Goizueta Foundation. The research was conducted at the Georgia Institute of Technology.

Disclosure statement

No potential conflict of interest was reported by the authors.

Notes

1. Email: dcortes@nmsu.edu
2. Email: Carlos.Santamarina@KAUST.edu.sa

References

AASHTO, 1993. *Guide for design of pavement structures*. Washington, DC: AASHTO.

Al-Qadi, I.L., Wang, H., and Tutumluer, E., 2010. Dynamic analysis of thin asphalt pavements by using cross-anisotropic stress-dependent properties for granular layer. *Transportation Research Record*, 2154 (1), 156–163. doi:10.3141/2154-16.

Alonso, E.E., 2003. Exploring the limits of unsaturated soil mechanics: The behavior of coarse granular soil and rockfill. *The 11th Buchanan Lecture*. University of Texas A&M.

Alonso, E.E., Pinyol, N.M., and Gens, A., 2012. Compacted soil behaviour: Initial state, structure and constitutive modelling. *Géotechnique*, 63 (6), 463–478.

Arthur, J.R.F. and Menzies, B.K., 1972. Inherent anisotropy in a sand. *Geotechnique*, 22 (1), 115–128. doi:10.1680/geot.1972.22.1.115.

Barden, L., 1963. Stresses and displacements in a cross-anisotropic soil. *Geotechnique*, 13 (3), 198–210. doi:10.1680/geot.1963.13.3.198.

Burmister, D.M., *et al.*, 1943. The theory of stress and displacements in layered systems and applications to the design of airport runwaysed. *Proceedings of the Twenty-Third Annual Meeting of the Highway Research Board Held at Edgewater Beach Hotel*, Chicago, IL, November 27–30.

Burmister, D.M., 1945. The general theory of stresses and displacements in layered systems. I. *Journal of Applied Physics*, 16 (2), 89–94. doi:10.1063/1.1707558.

Cascante, G. and Santamarina, J.C., 1996. Interparticle contact behavior and wave propagation. *Journal of Geotechnical Engineering*, 122 (10), 831–839. doi:10.1061/(ASCE)0733-9410(1996)122:10(831).

Cha, M., *et al.*, 2014. Small-strain stiffness, shear-wave velocity, and soil compressibility. *Journal of Geotechnology Geoenvironmental Engineering*, 140 (10), 06014011.

Cho, G.C. and Santamarina, J.C., 2001. Unsaturated particulate materials-particle-level studies. *Journal of Geotechnical and Geoenvironmental Engineering*, 127 (1), 84–96. doi:10.1061/(ASCE)1090-0241(2001)127:1(84).

Cortes, D.D. and Santamarina, J.C., 2013. The lagrange case history: Inverted pavement system characterisation and preliminary numerical analyses. *International Journal of Pavement Engineering*, 14 (5), 463–471. doi:10.1080/10298436.2012.742192.

Dai, S., Wuttke, F., and Santamarina, J.C., 2011. Coda wave analysis to monitor processes in soils. *Journal of Geotechnical and Geoenvironmental Engineering*, 139 (9), 1504–1511.

Einav, I., 2007. Breakage mechanics—part ii: Modelling granular materials. *Journal of the Mechanics and Physics of Solids*, 55 (6), 1298–1320. doi:10.1016/j.jmps.2006.11.004.

Fhwa, 1996. *Resilient modulus of unbound granular base/subbase materials and subgrade soils long-term pavement performance protocol 46*. Federal Highway Administration Pavement Performance Division.

Fleming, P.R., Frost, M.W., and Lambert, J.P., 2007. Review of lightweight deflectometer for routine in situ assessment of pavement material stiffness. *Transportation Research Record: Journal of the Transportation Research Board*, 2004 (1), 80–87. doi:10.3141/2004-09.

Fleming, P.R., Frost, M.W., and Rogers, C.D.F., 2000. A comparison of devices for measuring stiffness in situ. *Unbound aggregates in road construction: Proceedings of the Fifth International Symposium on Unbound Aggregates in Roads*, UNBAR 5, Nottingham, UK. pp. 193–200.

Fox, W.E.A. and Acum, L., 1951. Computation of load stresses in a three-layer elastic system. *Geotechnique*, 2 (4), 293–300. doi:10.1680/geot.1951.2.4.293.

Gazetas, G., 1982. Stresses and displacements in cross-anisotropic soils. *Journal of the Geotechnical Engineering Division*, 108 (4), 532–553.

Hicks, R.G. and Monismith, C.L., 1971. Factors influencing the resilient response of granular materials. *Highway Research Record* (345), 15–31.

Hossain, Z., *et al.*, 2007. Dem analysis of angular ballast breakage under cyclic loading. *Geomechanics and Geoengineering: An International Journal*, 2 (3), 175–181. doi:10.1080/17486020701474962.

Kim, I.T. and Tutumluer, E., 2005. Unbound aggregate rutting models for stress rotations and effects of moving wheel loads. *Transportation Research Record: Journal of the Transportation Research Board*, 1913 (1), 41–49. doi:10.3141/1913-05.

Kim, S.-H., Little, D.N., and Masad, E., 2005. Simple methods to estimate inherent and stress-induced anisotropy of aggregate base. *Transportation Research Record: Journal of the*

Transportation Research Board, 1913 (1), 24–31. doi:10.3141/1913-03.

Kopperman, S.E., Stokoe, K.H., and Knox, D.P., 1982. Effect of state of stress on velocity of low-amplitude compression waves propagating along principal stress directions in dry sand. Technical report, US Air Force Office of Scientific Research.

Lewis, D.E., *et al.*, 2012. Construction and performance of inverted pavements in Georgia. TRB 91st Annual Meeting, Available from: http://amonline.trb.org/1sgra7/1

Lu, N. and Likos, W.J., 2004. *Unsaturated soil mechanics*. New York: Wiley.

Mcdowell, G., Bolton, M., and Robertson, D., 1996. The fractal crushing of granular materials. *Journal of the Mechanics and Physics of Solids*, 44 (12), 2079–2101. doi:10.1016/S0022-5096(96)00058-0.

Nazarian, S., Baker, M.R., and Crain, K., 1993. Development and testing of a seismic pavement analyzer. Report, Strategic Highway Research Program, National Academy of Sciences.

NCHRP, 2002. Recommended standard method for routine resilient modulus testing of unbound granular base/subbase materials and subgrade soils, protocol 1-28a. National Cooperative Highway Research Program, Washington, DC.

NCHRP, 2004. *Guide for mechanistic-empirical design of new and rehabilitated pavement structures*. National Cooperative Highway Research Program, Transportation Research Board, Washington, DC.

NCHRP, 2008. *NCHRP synthesis 381: falling weight deflectometer usage*. Washington, DC: U.S. Department of the Interior.

Papadopoulos, E., 2014. *Performance of unbound aggregate bases and implications for inverted base pavements*. Atlanta, GA: Georgia Institute of Technology.

Papadopoulos, E. and Santamarina, J.C., 2014. Optimization of inverted base pavement designs with thin asphalt surfacing. *In*: *Geo-congress 2014 technical papers*. Atlanta, GA: ASCE, 2996–3004.

Papadopoulos, E. and Santamarina, J.C., 2015. Analysis of inverted base pavements with thin asphalt layers. *International Journal of Pavement Engineering*. Published online, doi:10.1080/10298436.2015.1007232.

Puppala, A.J., 2008. *Estimating stiffness of subgrade and unbound materials for pavement design*. Washington, DC: Transportation Research Board.

Roesler, S.K., 1979. Anisotropic shear modulus due to stress anisotropy. *Journal of the Geotechnical Engineering Division*, 105 (7), 871–880.

Santamarina, J.C. and Cascante, G., 1996. Stress anisotropy and wave propagation: A micromechanical view. *Canadian Geotechnical Journal*, 33 (5), 770–782. doi:10.1139/t96-102-323.

Santamarina, J.C. and Fratta, D., 2005. *Discrete signals and inverse problems*. Chichester: Wiley.

Santamarina, J.C., Klein, K., and Fam, M.A., 2001. *Soils and waves: Particulate materials behavior, characterization and process monitoring*. New York: Wiley.

Schuettpelz, C.C., Fratta, D., and Edil, T.B., 2010. Mechanistic corrections for determining the resilient modulus of base course materials based on elastic wave measurements. *Journal of Geotechnical and Geoenvironmental Engineering*, 136 (8), 1086–1094. doi:10.1061/(ASCE)GT.1943-5606.0000329.

Siripun, K., Jitsangiam, P., and Nikraz, H., 2011. The effects of moisture characteristics of crushed rock base (crb). *In*: *Geo-Frontiers 2011: Advances in Geotechnical Engineering*, Mar 13–15. Dallas, TX: American Society of Civil Engineers (ASCE). pp. 4458–4467.

Snieder, R., *et al.*, 2002. Coda wave interferometry for estimating nonlinear behavior in seismic velocity. *Science*, 295 (5563), 2253–2255. doi:10.1126/science.1070015.

Snieder, R., 2006. The theory of coda wave interferometry. *Pure and Applied Geophysics*, 163 (2–3), 455–473. doi:10.1007/s00024-005-0026-6.

Terrell, R.G., 2002. Measuring directional stiffnesses in pavement base material, Ph.D. Thesis, University of Texas, Austin.

Terrell, R.G., *et al.*, 2003. Field evaluation of the stiffness of unbound aggregate base layers in inverted flexible pavements. *Transportation Research Record*, 1837 (1), 50–60. doi:10.3141/1837-06.

Tutumluer, E., 2013. *Practices for unbound aggregate pavement layers*. NCHRP Synthesis 445, Transportation Research Board, Washington, DC.

Tutumluer, E. and Seyhan, U., 1999. Laboratory determination of anisotropic aggregate resilient moduli using an innovative test device. *Transportation Research Record*, 1687 (1), 13–21. doi:10.3141/1687-02.

Wang, H. and Al-Qadi, I.L., 2013. Importance of nonlinear anisotropic modeling of granular base for predicting maximum viscoelastic pavement responses under moving vehicular loading. *Journal of Engineering Mechanics*, 139 (1), 29–38. doi:10.1061/(ASCE)EM.1943-7889.0000465.

Williams, R.R. and Nazarian, S., 2007. Correlation of resilient and seismic modulus test results. *Journal of Materials in Civil Engineering*, 19 (12), 1026–1032. doi:10.1061/(ASCE)0899-1561(2007)19:12(1026).

Yimsiri, S. and Soga, K., 2002. Application of micromechanics model to study anisotropy of soils at small strains. *Soils and Foundations*, 42 (5), 15–26. doi:10.3208/sandf.42.5_15.

Yuan, D. and Nazarian, S., 2003. Variation in moduli of base and subgrade with moistureed. *In*: *Transportation Research Board 82nd Annual Meeting*, Washington, DC.